Optimized design of next-generation multiplexing schemes for GNSSs

IET Radar, Sonar & Navigation

Special Issue Call for Papers

Be Seen. Be Cited.
Submit your work to a new IET special issue

Connect with researchers and experts in your field and share knowledge.

Be part of the latest research trends, faster.

Read more

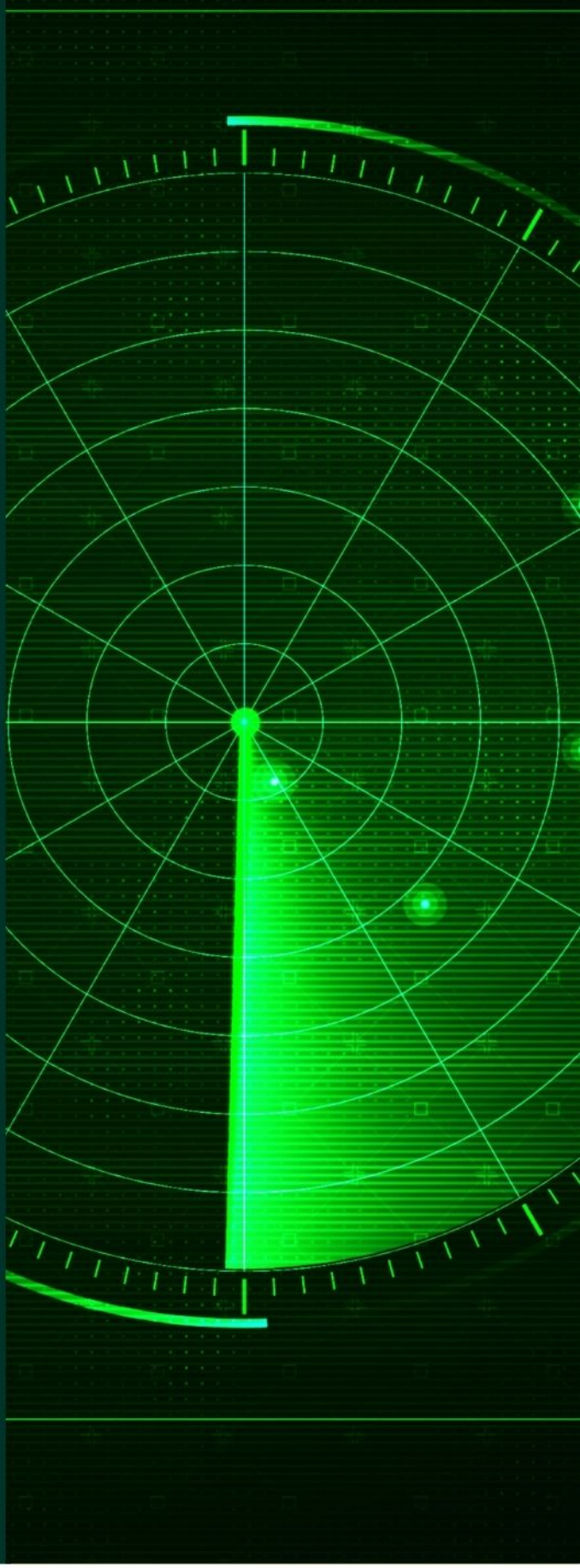

The Institution of Engineering and Technology

Received: 1 February 2023 | Revised: 21 March 2023 | Accepted: 29 March 2023

DOI: 10.1049/rsn2.12403

IET Radar, Sonar & Navigation

The Institution of Engineering and Technology WILEY

ORIGINAL RESEARCH

Optimised design of next-generation multiplexing schemes for Global Navigation Satellite Systems

Andrea Nardin[1] | **Fabio Dovis**[1] | **Simone Perugia**[2] | **Calogero Cristodaro**[2] | **Vittorio Valle**[2]

[1]Department of Electronics and Telecommunications, Politecnico di Torino, Turin, Italy

[2]Domain Observation and Navigation Italy (DONI), Thales Alenia Space Italy, Rome, Italy

Correspondence

Andrea Nardin.
Email: andrea.nardin@polito.it

Abstract

Multilevel and multicarrier component signals are now common in many Global Navigation Satellite Systems challenging the employed multiplexing method that needs to be more flexible and powerful. In this work, the authors demonstrate how, by acting on two parameters of the digital baseband representation of component signals (the sampling frequency and the central frequency of the baseband complex envelope), it is possible to optimise the performance of the multiplexer, while still obtaining a composite signal that fulfils the required system constraints.

KEYWORDS

global positioning system, satellite navigation, radionavigation

1 | INTRODUCTION

Nowadays, every Global Navigation Satellite System (GNSS), such as the Global Positioning System, Galileo, GLONASS, and BeiDou, provides multiple positioning, navigation and timing (PNT) services to its users [1]. An important feature that is also adopted by smaller regional navigation systems such as the Quasi-Zenith Satellite System and NavIC [1]. This diversified offer is ultimately enabled by the simultaneous broadcasting of several signals. However, the transmission of the resulting extended signal set needs to cope with the limited resource availability of a satellite's payload. In particular, it is desirable that the continuous transmission of different signals is performed throughout the same transmission chain (frequency up-converter, amplifier chain, and antenna) for the economical use of resources. The combination of these *component signals* into a *composite signal* over a shared medium is called *signal multiplexing*. Generally, in the satellite communications domain, the composite signal should exhibit a constant envelope (CE), to enable the high power amplifier (HPA) to operate at saturation, thus maximising the power efficiency while preventing signal distortions. Besides CE, GNSS multiplexing methods should guarantee backward and forward compatibility to globally widespread receivers, that is, they should be *transparent* to users [2]. Additionally, the necessary power loss employed to obtain a CE signal should be kept at its lowest, thus maximising what is termed as the *multiplexing efficiency* [2–4].

PNT is made possible by GNSSs through the broadcasting of orthogonal bipolar spreading chip waveforms transmitted over the same carrier, but in the last decades, the evolution of PNT services has brought in more complex waveforms. Multilevel spreading chips have been proposed to achieve better ranging accuracy [5]. On the other hand, the growing number of services have also been allocated to adjacent carriers, [1] and the combination of these signals into a single composite multicarrier signal has become attractive to limit the number of amplifier chains [6] and to foster innovative receiver processing strategies [7, 8]. Nonetheless, the emerging low earth orbit PNT paradigm [8–10] is encouraging a flexible PNT signals generation on payloads designed for rapid reconfiguration [9]. In this variegated scenario, with signals becoming more complex and diverse, the need for highly flexible and generalised signal multiplexing design has grown [4].

Multilevel and multicarrier waveforms are characterised by an increased number of possible values of amplitude and phase. This fact raises the complexity of the multiplexing algorithm, which has to satisfy the aforementioned constraints (CE and transparency) for a large number of combinations

of signal values while limiting the possible multiplexing efficiency reduction [2]. However, the number of signal value combinations—and more generally the multiplexer performance—is a consequence of the digital representation of the signal. The values taken by the digital samples when generated at baseband are strictly dependent on two parameters—the *central frequency* f_c with respect to which the baseband components are generated and the sampling frequency f_s—and both can be freely set to some extent, yielding an equivalent analogue Radio Frequency (RF) signal. Nonetheless, their choice impacts the complexity that the multiplexing algorithm has to face.

In this letter, we show how optimal f_c and f_s can improve the multiplexing efficiency with or without the knowledge of the multiplexing method. Specifically, these novel results show that these parameters have a large impact on variegated signal ensembles, promoting this flexible design approach to well-suit the needs of next-generation GNSSs and PNT services.

2 | THE MULTIPLEXING PROBLEM IN GLOBAL NAVIGATION SATELLITE SYSTEM

Let's consider a set of N orthogonal signal components $\tilde{s}_i(t)$ transmitted at several carrier frequencies $f_{i,\mathrm{RF}}$. Ideally, the resulting RF signal should be

$$s_{\mathrm{RF}}(t) = \sum_{i=1}^{N} \Re\left\{ \sqrt{P_i}\, e^{j\phi_i} \tilde{s}_i(t) e^{j2\pi f_{i,\mathrm{RF}} t} \right\} \tag{1}$$

where P_i and ϕ_i are the relative power and phase, respectively, assigned to the ith component by system design. A GNSS multiplexing scheme combines the $\tilde{s}_i(t)$ waveforms on both the in-phase and quadrature components of a single transmission chain, allowing to write the modulated signal as follows:

$$s_{\mathrm{RF,MUX}}(t) = \Re\left\{ s_{\mathrm{MUX}}(t) e^{j2\pi f_{\mathrm{RF}} t} \right\} \tag{2}$$

where $s_{\mathrm{MUX}}(t)$ is a complex envelope of the modulated signal when a f_{RF} down-conversion is used, as depicted in Figure 1. The modulated signal $s_{\mathrm{RF,MUX}}(t)$ has a power spectral density, which retains the spectral properties of $s_{\mathrm{MUX}}(t)$ shifted by f_{RF}. So to approach equation (1), the relative frequency separation among components should also be preserved in the baseband signal $s_{\mathrm{MUX}}(t)$.

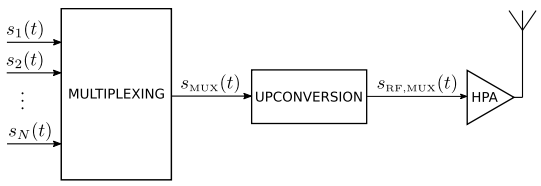

FIGURE 1 Multiplexer and high-level transmission chain.

In GNSS applications, the orthogonality of the components $\tilde{s}_i(t)$ allows the receiver to treat them separately through a correlation operation. Hence, a straightforward way to multiplex orthogonal signals is by direct superposition (DS), obtaining

$$s_{\mathrm{DS}}(t) = \sum_{i}^{N} \sqrt{P_i} e^{j\phi_i} \tilde{s}_i(t) e^{j2\pi f_i t} \tag{3}$$

where we set

$$f_i = f_{i,\mathrm{RF}} - f_{\mathrm{RF}}. \tag{4}$$

If $s_{\mathrm{MUX}}(t) = s_{\mathrm{DS}}(t)$, then $s_{\mathrm{RF,MUX}}(t) = s_{\mathrm{RF}}(t)$ is readily obtained through equation (2). More generally, $s_{\mathrm{RF,MUX}}(t) \approx s_{\mathrm{RF}}(t)$ as long as $s_{\mathrm{MUX}}(t) \approx s_{\mathrm{DS}}(t)$. However, for a generic set of signals $s_i(t) = \tilde{s}_i(t) e^{j2\pi f_i t}$ there are no obvious values for f_i. Indeed, while $f_{i,\mathrm{RF}}$ is usually imposed by system design, f_{RF} can be freely set. In a digitised transmitter, for instance, we can assign $f_i = 0$ to an arbitrary ith component as long as its relative frequency separation with the other signals is maintained and the subsequent RF modulation is performed according to equation (4). We can write

$$f_{i,\mathrm{RF}} = f_i + f_{\mathrm{RF}} \tag{5}$$

$$= f_i - f_c + f_{\mathrm{RF}} + f_c \tag{6}$$

$$= f'_i + f'_{\mathrm{RF}} \tag{7}$$

and notice that the use of $f_i = f'_i$ in $s_i(t)$ would lead to a new composite signal $s_{\mathrm{MUX}}(t)'$ represented with respect to a common frequency offset f_c. Nonetheless, the use of $f_{\mathrm{RF}} = f'_{\mathrm{RF}}$ would result in a modulated signal $s_{\mathrm{RF,MUX}}(t)'$, which is also an approximation of equation (1) as illustrated in Figure 2. From the signal generation perspective, there is no obvious choice of f_c.

To cope with the non-linearity of the HPA, the multiplexer has to provide a signal $s_{\mathrm{MUX}}(t) = A(t)e^{j\theta(t)}$ that after the upconversion to f_{RF} passes through the HPA with minimum distortions and power loss, that is, a CE signal, with $A(t) = A$.

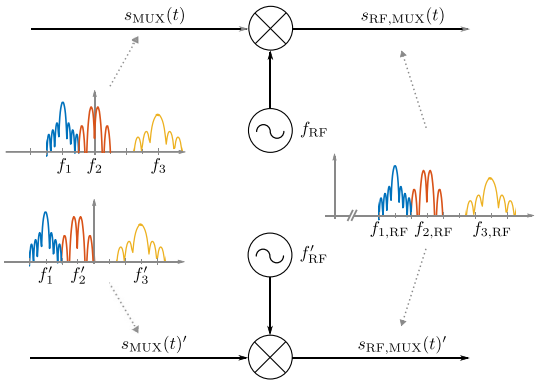

FIGURE 2 Equivalent frequency upconversion blocks.

To satisfy transparency, the orthogonality among the signal components has to be preserved, so that the component's power and phase can be recovered at the receiver side for every component i. This is done through a correlation operation whose output can be modelled as expressed below:

$$R_i = \frac{1}{T_i}\int_{T_i} s_{\mathrm{MUX}}(t)s_i(t)^*\mathrm{d}t \approx \sqrt{P_i}e^{j\phi_i} \tag{8}$$

for some integration interval T_i. The approximation is motivated by generally non-perfectly orthogonal signals.

We can formalise the GNSS multiplexing problem as finding a mapping function $\Omega : \{s_1(t), \ldots, s_N(t)\} \rightarrow s_{\mathrm{MUX}}(t)$ subject to the conditions

$$\sqrt{P_i}e^{j\phi_i} = \frac{1}{T_i}\int_{T_i} s_{\mathrm{MUX}}(t)s_i(t)^*\mathrm{d}t \quad \forall\, i \tag{9}$$

$$s_{\mathrm{MUX}}(t) = Ae^{j\theta(t)}. \tag{10}$$

Using DS would satisfy (9), but the envelope of $s_{\mathrm{DS}}(t)$ is generally non constant. It is also desirable to maximise the multiplexing efficiency [3]

$$\eta = \frac{\sum_{i=1}^{N}|R_i|^2}{A^2}. \tag{11}$$

Maximising (11) means that the sum of the components' power measured at the correlator's output should be as close as possible to the power of the composite signal. The power gap between $s_{\mathrm{MUX}}(t)$ and the sum of useful components corresponds to the power employed by the multiplexer to transform $s_{\mathrm{DS}}(t)$ to a CE signal. Such a relationship can be written as given below [2]:

$$s_{\mathrm{MUX}}(t) = s_{\mathrm{DS}}(t) + s_{\mathrm{AUX}}(t) \tag{12}$$

where $s_{\mathrm{AUX}}(t)$ represents an auxiliary component. Note that not all the multiplexing algorithms explicitly compute $s_{\mathrm{AUX}}(t)$, but the process can be described through equation (12) in the vast majority of cases [2].

3 | INPUT OPTIMISATION FOR MULTIPLEXING

In a digital implementation, a multilevel multicarrier signal component can be defined by the following equation:

$$s_i[n] = \sum_{k=-\infty}^{+\infty} c_k^{(i)} p_i\left(\frac{n}{f_s} - kT_c^{(i)}\right)e^{j2\pi f_i\frac{n}{f_s}} \tag{13}$$

where $c_k^{(i)}$ is the kth bipolar spreading symbol determined by the chip sequence and navigation data, and p_i is the pulse shape of the chip of duration $T_c^{(i)}$. It is clear from (13) that given a pulse shape for the ith component, the set of possible values of $s_i[n]$ is determined by f_s and f_i. As multiple signal components are combined, the mapping Ω has to establish a relation between the value of the composite signal $s_{MUX}(t)$ and every different set of values that the signals in $\{s_1[n], \ldots, s_N[n]\}$ can assume. Therefore, as the number and characteristics of these sets of combination values change, the complexity necessary to compute a feasible multiplexing mapping might increase. Thus, the resulting mapping has to satisfy equations (9) and (10), without disrupting the multiplexing efficiency performance. Indeed, f_s can be arbitrarily chosen as long as the Nyquist limit is observed and possible additional constraints imposed by the hardware are respected. Similarly, the central frequency shift f_c with respect to which each f_i is defined can be freely set and the signal components can be generated through equation (13) by updating f_i and f_{RF} in accordance with equations (6) and (7).

Given a set of signals, we can find the optimal baseband configuration that maximises the multiplexing efficiency. In other words, we need to find

$$\left(\widehat{f}_s, \widehat{f}_c\right) = \arg\max_{f_s, f_c} \eta. \tag{14}$$

The multiplexing efficiency is affected by f_s and f_c but is also determined by both the component signals waveforms and the multiplexing algorithm, which parametrise the function. A relationship that can be expressed through a function g so that

$$\eta = g\left(f_s, f_c; s_1[n], \ldots, s_N[n], \Omega\right). \tag{15}$$

The complexity of multiplexing algorithms for multilevel and multicarrier signals generally prevents the derivation of an explicit analytical expression for equation (15). Instead, the optimisation must be done through an exhaustive search, by exploring the whole solution space to identify the pair (f_s, f_c) that provides the best configuration for a given set of signal waveforms. This approach is computationally expensive since a mapping function Ω must be derived for each tested pair to compute $s_{\mathrm{MUX}}(t)$ and the resulting η.

An alternative indicator of the multiplexing performance can be obtained from the original signal components alone. Indeed, the power loss spent to grant the CE of $s_{\mathrm{MUX}}(t)$, that is, the power of $s_{\mathrm{AUX}}(t)$, depends on how scattered the values of $|s_{\mathrm{DS}}(t)|$ are, which is measured by the *nonconstancy* metric defined in ref. [4]. Consider the *signal value vector* $\mathbf{s}_{\mathrm{DS}}$—a vector made of all the possible values assumed by $s_{\mathrm{DS}}[n] = \sum_{i=1}^{N}\sqrt{P_i}e^{j\phi_i}s_i[n]$, sorted in ascending order. Such a vector contains an even number of elements for bipolar spreading symbols. A measure of the initial non-constancy is given by the following equation:

$$C = \mathbf{s}_{\mathrm{DS}}^{\mathrm{H}}\mathbf{G}\mathbf{s}_{\mathrm{DS}} \tag{16}$$

where $\mathbf{G} = \mathrm{diag}(-1\cdots -1 + 1\cdots +1)$ is a diagonal matrix whose first half of the diagonal contains a sequence of -1 and the second half is made of $+1$. It is easy to show that C is a

non-negative scalar function and $C = 0$ if and only if all the elements in $|\mathbf{s}_{DS}|$ are equal. We can thus use equation (16) as a measure of how far a sum of signal components is from a CE configuration. The initial lack of constancy does not depend on the multiplexing algorithm Ω, but it is still related to the resulting multiplexing efficiency. We can express its optimisation as given below:

$$\left(\widehat{f}_s, \widehat{f}_c\right) = \underset{f_s, f_c}{\arg\min}\, C \tag{17}$$

noting that

$$C = h\left(f_s, f_c; s_1[n], \ldots, s_N[n]\right) \tag{18}$$

for an unknown function h that is not parametrised by Ω. Through this approach, we can eventually find the optimal f_s and f_c to get an initial set of signals whose sum is the closest to having a CE. This will likely result in a composite signal with a high multiplexing efficiency, but the final result will ultimately depend on the mapping Ω (i.e. the multiplexing method). For this reason, C can be just an indicator of the multiplexing efficiency, but its independence from the adopted multiplexing scheme makes it a promising performance metric based solely on the signals' configuration.

4 | RESULTS AND DISCUSSION

In this section, we analyse optimal f_s and f_c for a selected case study, that is, a specific set of component signals and a multiplexing method. To provide timely and relevant results, we implemented the algorithm named CE multiplexing via intermodulation construction (CEMIC), a state-of-the-art multicarrier solution that achieves the highest multiplexing efficiency among existing methods [4]. A set of signal components has been chosen in line with modern GNSSs with some adaptations, trying to challenge both the multiplexer and the input optimisation process. The signal characteristics and initial f_i values are summarised in Table 1 and the resulting PSDs are shown in Figure 3. Notice that the signal $s_1[n]$ has been designed to maximise its Gabor bandwidth and increase its ranging accuracy [5] according to the well-known Cramér–Rao bound for time-delay estimation [1]. Its chip is defined by the sequence $p_1 = (-0.2, 0.375, -0.4, 0.5, -0.5, 0.4, -0.375, 0.2)$.

An exhaustive search of the best (f_s, f_c) pair in terms of multiplexing efficiency led to the results in Figure 4. The search has been performed with a step size of $f_0 = 1.023$ MHz along both dimensions. Several configurations provide high multiplexing efficiency values, but the overall best is reported in Table 2 for the corresponding objective function. The nearly constant η values that can be found along the f_c direction in Figure 4 suggest that some values of f_s negatively affect the multiplexing optimisation process, regardless of the chosen f_c. This could lead to a multiplexing efficiency power loss of up to 21.25%. Furthermore, as f_s increases, η exhibits generally lower values. Due to the presence of offset carriers, a high sampling frequency in equation (13) leads to a large number of possible signal values for which the multiplexing algorithm is less likely to be efficient in providing a CE signal.

We repeated the analysis over the same search space by assessing the initial constancy for each configuration. For this investigation, we built the signal value vector $\mathbf{s}_{DS}$ to measure the non-constancy through equation (16). The resulting values

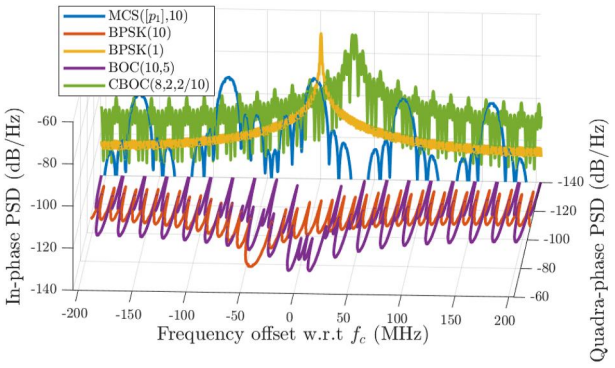

FIGURE 3 Component signals estimated power spectral density (PSD).

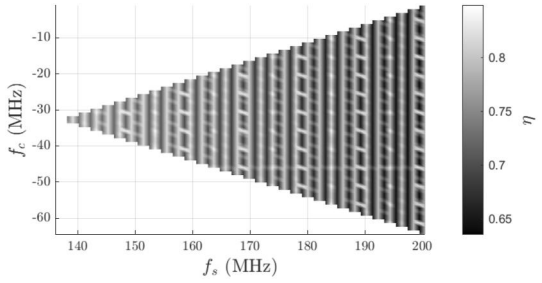

FIGURE 4 Multiplexing efficiency η with respect to f_s and f_c. Missing values are due to a resulting signal band sampled under the Nyquist limit.

TABLE 1 Component signals initial configuration

Component	Modulation[a]	Initial offset carrier[b] f_i	Phase	Power
s_1	MCS ($[p_1]$,10)	$-45f_0$	I	0.10
s_2	BPSK (10)	$-45f_0$	Q	0.15
s_3	BPSK (1)	0	I	0.10
s_4	BOC (10,5)	0	Q	0.30
s_5	CBOC (8,2,2/10)	$+30f_0$	I	0.35

[a]The modulations are multilevel coded symbols (MCS), binary phase shift keying (BPSK), binary offset carrier (BOC), and composite binary offset carrier (CBOC) [11].
[b]Defined as multiple of $f_0 = 1.023$ MHz.

TABLE 2 Component signals configuration

Objective function	Optimal f_s	Optimal f_c	η[a]
η	$150f_0$	$-30f_0$	0.848
C	$150f_0$	$-30f_0$	0.848

[a]Multiplexing efficiency obtained using optimal f_s and f_c for signals generation.

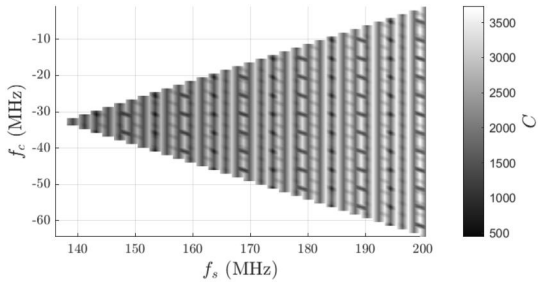

FIGURE 5 Non-constancy C with respect to f_s and f_c.

of C are shown in Figure 5 and the corresponding optimal pair is reported in Table 2. The minimisation of C led to the same (f_s, f_c) pair with respect to the previous experiment, corresponding to the same η value. Moreover, it can be noticed that the two plots of Figures 4 and 5 exhibit a similar trend. Indeed, an analysis of the correlation among the computed values of η and C, performed through the Pearson correlation coefficient, showed that there is a correlation among these two variables of -0.99 for the case under study. This means that for a given signal component configuration when C is small, there is a high chance that the multiplexing efficiency of the resulting signal $s_{\mathrm{MUX}}(t)$ will be large and vice versa. The ultimate result depends on the chosen multiplexing method. However, it is reasonable to assume that a similar relationship holds for every multiplexing method as long as its mapping process can be described by equation (12).

5 | CONCLUSION

We saw that a bad choice of f_s and f_c can severely affect the multiplexing performance (Figure 4) causing a power loss of more than 20%. Moreover, as highlighted by Figure 4, a low f_s should be preferred using multicarrier signals as it can largely worsen the multiplexer's performance. Avoiding such poorly performing configurations motivates this input optimisation analysis, which eventually provided non-trivial optimal solutions like the ones in Table 2. Moreover, a solution based on the overall constancy of the component signals configuration has been obtained. This solution is agnostic about the multiplexing method, having therefore a general significance, but is also not optimal in the multiplexing efficiency sense. Nonetheless, we found it to be an accurate indicator of the latter by measuring a correlation coefficient between the two objective functions of -0.99 for the case under study.

AUTHOR CONTRIBUTIONS

Andrea Nardin: Conceptualisation; Data curation; Formal-analysis; Investigation; Methodology; Resources; Software; Supervision; Validation; Visualisation. **Fabio Dovis**: Conceptualisation; Funding acquisition; Supervision; Writing—review & editing. **Simone Perugia**: Conceptualisation; Writing—review & editing. **Calogero Cristodaro**: Writing—review & editing. **Vittorio Valle**: Writing—review & editing

CONFLICT OF INTEREST STATEMENT

None

DATA AVAILABILITY STATEMENT

The data that support the findings of this study are available from the corresponding author upon reasonable request.

ORCID

Andrea Nardin https://orcid.org/0000-0001-9167-2272
Fabio Dovis https://orcid.org/0000-0001-6078-9099
Simone Perugia https://orcid.org/0000-0001-8804-1314
Calogero Cristodaro https://orcid.org/0000-0003-0299-3918
Vittorio Valle https://orcid.org/0000-0003-0589-5838

REFERENCES

1. Teunissen, P., Montenbruck, O.: Springer Handbook of Global Navigation Satellite Systems, 1st ed. Springer. Cham (2017)
2. Yao, Z., Lu, M.: Signal multiplexing techniques for GNSS: the principle, progress, and challenges within a uniform framework. IEEE Signal Process. Mag. 34(5), 16–26 (2017). https://doi.org/10.1109/msp.2017.2713882
3. Dafesh, P.A., Cahn, C.R.: Phase-optimized constant-envelope transmission (POCET) modulation method for GNSS signals. In: Proceedings of the 22nd International Technical Meeting of the Satellite Division of the Institute of Navigation (ION GNSS 2009), pp. 2860–2866 (2009)
4. Yao, Z., et al.: Orthogonality-based generalized multicarrier constant envelope multiplexing for DSSS signals. IEEE Trans. Aero. Electron. Syst. 53(4), 1685–1698 (2017). https://doi.org/10.1109/taes.2017.2671580
5. Zhang, X., Yao, Z., Lu, M.: Optimizing the Gabor bandwidth of satellite navigation signals by MCS signal expression. Sci. China Phys. Mech. Astron. 54(6), 1077–1082 (2011). https://doi.org/10.1007/s11433-011-4329-6
6. Yao, Z., Lu, M.: Dual-frequency constant envelope multiplex with non-equal power allocation for GNSS. Electron. Lett. 48(25), 1624–1625 (2012). https://doi.org/10.1049/el.2012.2952
7. Nardin, A., Dovis, F., Motella, B.: Impact of non-idealities on GNSS meta-signals processing. In: 2020 European Navigation Conference (ENC), pp. 1–8 (2020)
8. Nardin, A., Dovis, F., Fraire, J.A.: Empowering the tracking performance of LEO PNT by means of meta-signals. In: 2020 IEEE International Conference on Wireless for Space and Extreme Environments (WiSEE), pp. 153–158 (2020)
9. Iannucci, P.A., Humphreys, T.E.: Economical fused LEO GNSS. In: 2020 IEEE/ION Position, Location and Navigation Symposium (PLANS), pp. 426–443 (2020)
10. Nardin, A., Dovis, F., Fraire, J.A.: Empowering the tracking performance of LEO-based positioning by means of meta-signals. IEEE J. Radio Freq. Identif. 5(3), 244–253 (2021). https://doi.org/10.1109/jrfid.2021.3077082
11. Rodríguez, J.Á.Á.: On Generalized Signal Waveforms for Satellite Navigation. [dissertation]. Universität der Bundeswehr München (2008)

How to cite this article: Nardin, A., et al.: Optimised design of next-generation multiplexing schemes for Global Navigation Satellite Systems. IET Radar Sonar Navig. 17(7), 1100–1104 (2023). https://doi.org/10.1049/rsn2.12403